Journal of Magnetic Resonance **156,** 171–180 (2002)
doi:10.1006/jmre.2002.2541

# Enhanced Transverse Relaxation in Porous Media due to Internal Field Gradients

Keh-Jim Dunn

*ChevronTexaco Exploration and Production Technology Company, San Ramon, California 94583*

Received May 7, 2001; revised February 28, 2002; published online June 20, 2002

**We present a detailed comparison between the theoretically computed spin echo decay of a fluid-saturated periodic porous medium with strong internal field gradients and that obtained from various approximations using the free diffusion formula which is strictly valid only for infinite uniform fluids. The theoretical computation of the spin echo amplitude was carried out by using the diffusion eigenstates in Fourier representation, and the internal field gradients induced by magnetic susceptibility contrast were calculated by using a two-component composite theory. The comparison allows us to have an assessment of the regime of validity of various approximations for a periodic porous medium where a rigorous theoretical computation of the enhanced transverse relaxation due to magnetic susceptibility contrast induced field heterogeneity is possible.** 

## INTRODUCTION

There have been many papers (*1–10*) recently discussing the internal field gradients within the pore space of a porous medium due to magnetic susceptibility contrast between the solid matrix and the pore fluid. Most of them use the free diffusion formula (strictly valid only for infinite uniform fluids with a constant field gradient), i.e.,

$$\exp\left(-\frac{2\tau}{T_2}-\frac{2}{3}\gamma^2(\nabla H)^2 D_p \tau^3\right), \qquad [1]$$

to describe the enhanced $T_2$ relaxation in a porous medium, where $\tau$ is half the echo spacing, $\gamma$ is the gyromagnetic ratio, $D_p$ is the diffusion coefficient of the pore fluid, and $\nabla H$ is the field gradient. The volume integral of Eq. [1] was then used to represent the overall spin echo amplitude in a porous medium where strong internal gradients exist (*1, 2*).

The procedure of the volume integration was based on the thought that the observed signal in such a system can be considered as a superposition of individual microdomains, each of which has an effective field gradient. Hürlimann (*6, 7*) pointed out that there is a field averaging effect due to spin diffusions in heterogeneous fields and that there are several length scales one has to consider in the analysis of the magnetization decays. Dunn *et al.* (*10*) reviewed the detailed steps in analyzing the regular CPMG echo trains and inverting them to obtain the distributions of the internal field gradients of the pore space, and the various assumptions that one has to make in carrying out these analyses. However, they did not address the issue of how good the approximation is for this volume integration of signals from microdomains.

This question can be answered for a fluid-saturated porous medium if one can compute the spin echo amplitude rigorously for such a system and the result is compared with that obtained using the volume integration of microdomains. However, the computation of the spin echo amplitude decay affected by bounded diffusion in a restricted geometry is a very complicated matter. Early work by Neuman (*11*) assumed a Gaussian phase distribution and only computed the spin magnetizations for simple geometries such as parallel plates and spherical and cylindrical pores. Other work (*3, 12, 13*) discussed only the asymptotic behaviors at short and long times for spin diffusion in porous media of general shapes.

Later work by Bergman and Dunn (*14*), however, showed that it is possible to provide a complete description on the spin diffusion in a periodic porous medium in the presence of a nonuniform magnetic field. The field gradients can be either fixed externally applied field gradients or internal field gradients induced by the magnetic susceptibility contrast between the solid matrix and the pore fluid. Such a description is possible because the diffusion propagator of spins diffusing in the pore space for the periodic porous medium can be worked out explicitly in terms of diffusion eigenstates in Fourier representation. Hence the spin echo amplitude decay for such a restricted geometry can be rigorously computed. Also, the magnetic field distribution within the pore space for such a system can be computed using well-known methods in composite medium theory.

With the known magnetic field distribution within the pore space, we can calculate the volume integration of the signals from microdomains using the free diffusion formula (Eq. [1]) to obtain the spin echo amplitude, a commonly used procedure which has never been examined. We can also compute the spin echo amplitude rigorously using the diffusion propagator. Thus we can make a comparison between results of the rigorous method and those obtained from approximate approaches. Such a comparison is essential because, while the spin echo amplitude



1090-7807/02 $35.00

computed by using diffusion propagator is exact, we cannot apply this method to general disordered media. The analysis of such a comparison will help us establish some guidelines for using the approximate approaches, as well as limitations where these approximations may fail.

In the following, we first review how the internal gradient is computed in the pore space for a periodic porous medium. Then we briefly outline how the spin echo amplitude in a periodic porous medium is calculated. This is followed by a numerical example for a periodic porous system of simple cubic arrays of touching spheres. We establish, for this periodic geometry, bounds within which the Gaussian phase approximation is valid. Using this numerical example, various approximate approaches are analyzed and compared with the rigorous result to elucidate their limitations and possible error they may cause.

## COMPUTATION OF INTERNAL GRADIENTS

Computing the magnetic field heterogeneities within the pore space of a porous medium induced by the magnetic susceptibility contrast between the solid matrix and pore space is a well-known problem and has been studied extensively in the past. It is identical to the classical problem of computing the effective dielectric constant of a two-component composite. When computing the effective dielectric constant of the composite, the electric field can be evaluated at every point of either phase of the composite. Similarly, the inhomogeneous magnetic field due to magnetic susceptibility contrast between the two components of the composite, i.e., solid matrix and pore fluid, can be evaluated in the same manner. There is abundant literature on this subject. Bergman (*15–18*), as well as others, have done extensive work in this area.

Let us consider a periodic porous medium made of simple cubic arrays of identical touching spheres, where the solid spheres have a magnetic susceptibility of $\chi_m$, and between the spheres the pore space is filled with a pore fluid having a magnetic susceptibility of $\chi_p$. It is shown in the Appendix that the local field deviation $\delta H_{\text{susc}}(\mathbf{r})$ from an externally applied field $H_0$ along the $z$ direction due to the magnetic susceptibility contrast between the solid matrix and pore fluid is given by

$$\delta H_{\text{susc}}(\mathbf{r}) = H_0 \frac{\partial \psi}{\partial z} \cong \frac{H_0}{s} \sum_{\mathbf{g}\neq 0} \cos^2(\mathbf{g}, \mathbf{e_z}) \theta_{\mathbf{g}} e^{i\mathbf{g}\cdot\mathbf{r}}, \qquad [2]$$

where $s = (1 + 4\pi\chi_m)/4\pi(\chi_m - \chi_p)$, $\psi$ is the periodic part of the magnetic scalar potential, $\mathbf{g}$ is the reciprocal lattice vector, $(\mathbf{g}, \mathbf{e_z})$ is the angle between $\mathbf{g}$ and the unit vector $\mathbf{e_z}$ along the $z$-axis, and $\theta_{\mathbf{g}}$ is the Fourier coefficient of the characteristic function $\theta$, as described in the Appendix.

From Eq. [2], the field strength at every point in the pore space can be calculated. The field gradient can also be directly computed as a function of spatial position

$$|\nabla \delta H(\mathbf{r})| = \left[ \left( \frac{\partial \delta H}{\partial x} \right)^2 + \left( \frac{\partial \delta H}{\partial y} \right)^2 + \left( \frac{\partial \delta H}{\partial z} \right)^2 \right]^{\frac{1}{2}}. \qquad [3]$$

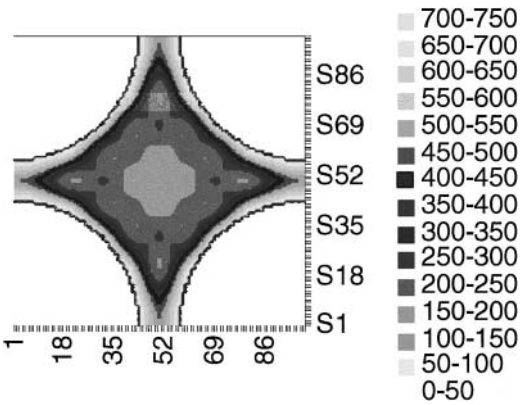


**FIG. 1.** The cross-sectional view (slightly above (100) plane) of the internal field gradient distribution in G/cm of a periodic porous medium of simple cubic arrays of touching spheres at an externally applied field of $H_0 = 234.9$ G (i.e., a proton Larmor frequency of 1 MHz), using $\chi_p = -0.7 \times 10^{-6}$ emu/cm$^3$ for the pore water, $\chi_m = 50 \times 10^{-6}$ emu/cm$^3$ for the solid matrix, and a unit cell size $a = 10$ $\mu$m for the periodic porous medium.

The volume average of $|\nabla \delta H(\mathbf{r})|^2$ can also be obtained as

$$\langle |\nabla \delta H(\mathbf{r})|^2 \rangle = \left( \frac{H_0}{s} \right)^2 \sum_{\mathbf{g}\neq 0} \cos^4(\mathbf{g}, \mathbf{e_z}) |\theta_{\mathbf{g}}|^2 |\mathbf{g}|^2. \qquad [4]$$

Using $\chi_p = -0.7 \times 10^{-6}$ emu/cm$^3$ for the pore water, $\chi_m = 50 \times 10^{-6}$ emu/cm$^3$ for the solid matrix, and a unit cell size of $a = 10$ $\mu$m, we computed the internal field gradient distribution within the pore space of a three-dimensional periodic system of simple cubic arrays of touching spheres at an externally applied field of $H_0 = 234.9$ G along the $z$ direction (i.e., a proton Larmor frequency of 1 MHz). The result is shown in Fig. 1 where the volume elements are color coded with internal field gradient values given in units of G/cm. Figure 2 shows the volume fraction

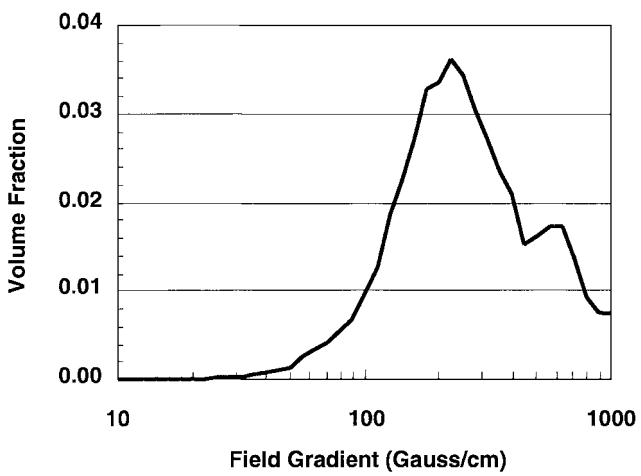


**FIG. 2.** The field gradient distribution in the pore space of a periodic porous system computed in Fig. 1.

having the same field gradient plotted as a function of the field gradient of the same calculation. A straight volume average of the field gradient gives an averaged value of 400 G/cm; the most probable value is about 200 G/cm. As we shall see, when the true spin echo amplitude is computed using the diffusion propagator, the effective (or apparent) field gradient is a function of diffusion time and is only about 100 G/cm at $\tau = 2$ ms. This is because, when a spin diffuses, there is a field averaging effect.

## CALCULATION OF SPIN ECHO AMPLITUDE

To calculate the spin echo amplitude, we know that the phase shift accumulated by a precessing spin in a Hahn's spin echo experiment with a local field deviation $\delta H$ is given by $\Phi$ as

$$\Phi = -\gamma\left(\int_0^{\tau} dt\,\delta H[\mathbf{r}(t)] - \int_{\tau}^{2\tau} dt\,\delta H[\mathbf{r}(t)]\right), \qquad [5]$$

where $\gamma$ is the gyromagnetic ratio and $\tau$ is the time duration for spin dephasing or rephasing (i.e., the time between the initial 90° pulse and the subsequent 180° pulse in a Hahn echo experiment). The average of the phase shift is obtained by integrating over all possible paths and all pore space with the aid of the diffusion propagator.

The phase average can be expressed as an expansion in cumulant averages of powers of $\Phi$ ($\langle\,\rangle_c$ represents a cumulant average):

$$\begin{aligned}\langle e^{-i\Phi}\rangle &= \exp\langle e^{-i\Phi} - 1\rangle_c \\ &= \exp\left[-i\langle\Phi\rangle_c - \frac{1}{2}\langle\Phi^2\rangle_c + \frac{i}{6}\langle\Phi^3\rangle_c + \frac{1}{24}\langle\Phi^4\rangle_c + \cdots\right].\end{aligned} \qquad [6]$$

It has been shown in Ref. (*14*) that any odd powers of $\Phi$ average to zero. When the distribution of values of $\Phi$ is Gaussian, all cumulants beyond $\langle\Phi^2\rangle_c$ vanish. For non-Gaussian distributions, the magnitudes of $\langle\Phi^4\rangle_c$ and higher order terms become a measure of the deviation from the Gaussian distribution. When $\langle\Phi^4\rangle_c$ and higher order terms are a significant fraction of $\langle\Phi^2\rangle_c$, the Gaussian approximation breaks down.

The theory for computing $\langle\Phi^2\rangle$ and $\langle\Phi^4\rangle$ in terms of the diffusion eigenstates was described in detail previously (*14, 19*). We shall briefly review the formulas of $\langle\Phi^2\rangle$ for effects of magnetic susceptibility contrasts and externally applied fixed gradient, and $\langle\Phi^4\rangle$ for magnetic susceptibility contrasts only. The other formulas for $\langle\Phi^4\rangle$ for applied fixed gradient and cross term are very lengthy. They are not reproduced here. Interested readers should refer to Ref. (*14*).

As discussed in Ref. (*14*), $\langle\Phi^2\rangle$ can be written as

$$\begin{aligned}\frac{1}{2\gamma^2}\langle\Phi^2\rangle = &\left(2\int_{\tau}^{2\tau} dt_2 \int_{\tau}^{t_2} dt_1 - \int_{\tau}^{2\tau} dt_2 \int_0^{\tau} dt_1\right) \\ &\cdot \langle\delta H[\mathbf{r}(t_2)]\delta H[\mathbf{r}(t_1)]\rangle.\end{aligned} \qquad [7]$$

The average over diffusion paths is

$$\begin{aligned}&\langle\delta H[\mathbf{r}(t_2)]\delta H[\mathbf{r}(t_1)]\rangle \\ &\quad = \frac{1}{V_p}\int_{V_p} dV_1 \int_{V_p} dV_2\, G(\mathbf{r}_2\mathbf{r}_1 \mid t_2 - t_1)\delta H(\mathbf{r}_2)\delta H(\mathbf{r}_1).\end{aligned} \qquad [8]$$

The diffusion propagator $G(\mathbf{r}\mathbf{r}' \mid t)$ is given by

$$G(\mathbf{r}\mathbf{r}' \mid t) = \frac{1}{V}\sum_{n\mathbf{q}} e^{-\lambda_{n\mathbf{q}}|t|}\phi_{n\mathbf{q}}(\mathbf{r})\phi^*_{n\mathbf{q}}(\mathbf{r}')e^{i\mathbf{q}\cdot(\mathbf{r}-\mathbf{r}')}, \qquad [9]$$

where $\lambda_{n\mathbf{q}}$ are the eigenvalues, $\phi_{n\mathbf{q}}(\mathbf{r})$ are the diffusion eigenstates, $q$ is a wave vector in the first Brillouin zone, $n$ is a band index, and $V$ is the total volume of the pore space and solid matrix.

Knowing $\delta H$ and $G(\mathbf{r}\mathbf{r}' \mid t)$ from Eqs. [2] and [9], and substituting both of them into Eqs. [7] and [8], we obtain the magnetic susceptibility contrast contribution to $\langle\Phi^2\rangle$ as given by

$$\langle\Phi^2\rangle_{\text{susc}} = \frac{2}{\phi}\left(\frac{\gamma H_0}{s}\right)^2 \sum_{n>0} b_n(\tau)|a_n|^2, \qquad [10]$$

where

$$b_n(\tau) \equiv \frac{2\tau}{\lambda_{n\mathbf{0}}} - \frac{1}{\lambda^2_{n\mathbf{0}}}\left(1 - e^{-\lambda_{n\mathbf{0}}\tau}\right)\left(3 - e^{-\lambda_{n\mathbf{0}}\tau}\right) \qquad \text{for } \lambda_{n\mathbf{0}} \neq 0 \qquad [11]$$

$$a_n \equiv \sum_{\mathbf{g}\neq 0} \cos^2(\mathbf{g}, \mathbf{e}_z)\theta^*_{\mathbf{g}}\tilde{\phi}_{n\mathbf{0}}(\mathbf{g}) \qquad [12]$$

$$\tilde{\phi}_{n\mathbf{0}}(\mathbf{g}) = \frac{1}{V_a}\int_{V_a} dV\,\theta_p(\mathbf{r})e^{-i\mathbf{g}\cdot\mathbf{r}}\phi_{n\mathbf{0}}(\mathbf{r}). \qquad [13]$$

The externally applied fixed gradient contribution to $\langle\Phi^2\rangle$ is given by

$$\begin{aligned}\langle\Phi^2\rangle_{\text{grad}} = &(\gamma\nabla H)^2\frac{4}{3}D_e\tau^3 + \frac{1}{\phi}\sum_{n>0} b_n(\tau) \\ &\times\left[\left(\gamma\nabla H\cdot\frac{\partial}{\partial\mathbf{q}}\right)^2 |\tilde{\phi}_{n\mathbf{q}}(\mathbf{0})|^2\right]_{\mathbf{q}=\mathbf{0}},\end{aligned} \qquad [14]$$

where $D_e$ is the effective diffusion coefficient at the long time limit for a restricted geometry.

The pure magnetic susceptibility contrast part of $\langle\Phi^4\rangle$ is given by

$$\frac{1}{24}\langle\Phi^4\rangle_{\text{susc}} = \frac{1}{\phi}(4\pi\Delta\chi\gamma H_0)^4 \sum_{n,m,l} b_{nml}(\tau)a_n a_{nm}a_{ml}a^*_l, \qquad [15]$$

where $a_n$ is given by Eq. [12], and

$$a_{nm} \equiv \sum_{\mathbf{g}\neq 0} \cos^2(\mathbf{g}, \mathbf{e_z})\theta^*_{\mathbf{g}}\omega_{nm}(\mathbf{g}) \quad [15]$$

$$\omega_{nm}(\mathbf{g}) \equiv \frac{1}{V_a}\int_{V_a\cap V_p} dV\phi^*_{n\mathbf{0}}(\mathbf{r})\phi_{m\mathbf{0}}(\mathbf{r})e^{-i\mathbf{g}\cdot\mathbf{r}} = \sum_{\mathbf{g}'}\tilde{\phi}^*_{n\mathbf{0}}(\mathbf{g}')\tilde{\phi}_{m\mathbf{0}}(\mathbf{g}+\mathbf{g}'). \quad [16]$$

The formulas for $b_{nml}(\tau)$ are quite lengthy and can be found in Ref. (*14*).

## BOUNDS FOR GAUSSIAN APPROXIMATION

Now that we know how to compute the internal gradients as well as compute the spin echo amplitude of a periodic porous medium exactly, we are in a position to evaluate various approximate formulas where the free diffusion equation (Eq. [1]) is used. We can, for example, examine the accuracy of the approach of the volume integration of microdomains.

There are various forms of approximations. First of all, we should realize that the volume average of the internal field gradients is not the same as the apparent field gradient obtained from using Eq. [1] in analyzing a set of CPMG data with a known diffusion coefficient and different $\tau$'s. The volume averaging of the internal field gradients is a linear operation, whereas the apparent field gradient in Eq. [1] is weighted exponentially. Thus replacing the field gradient term in Eq. [1] with the volume averaged field gradient is bound to overestimate the attenuation of the magnetization.

Second, for a space with magnetic field gradients, if we were to use Eq. [1] as the integrand to compute the total magnetization of the system in the following integral

$$\int d^3\mathrm{r}\exp\left[-\frac{2}{3}\gamma^2(\nabla H(\mathrm{r}))^2 D_p\tau^3\right] \quad [17]$$

or

$$\int dg\, P(g)\exp\left[-\frac{2}{3}\gamma^2 g^2 D_p\tau^3\right], \quad [18]$$

where $g$ is the field gradient (denoted as $\nabla H$ in Eq. [17] and previously), and $P(g)$ is the volume fraction having the field gradient $g$, we implicitly assume that each volume element of the integration behaves as if it is an isolated element which possesses the property of an infinite uniform medium, whereas in reality the spin diffuses freely among volume elements with very different values of field gradient.

Certainly, these approximations need re-evaluation to establish their bounds of validity. Before we do that, it is important to first establish the bounds of validity for the Gaussian phase approximation. For a system of simple cubic arrays of touching spheres, where the interstitial space is filled with water, we have computed the values of $\frac{1}{2}\langle\Phi^2\rangle_c$ and $\frac{1}{24}\langle\Phi^4\rangle_c$ for the diffusing spin in the pore space as a function of $\tau$. For convenience, we shall define the time when the absolute value of the ratio $\frac{1}{24}\langle\Phi^4\rangle_c/\frac{1}{2}\langle\Phi^2\rangle_c$ reaches 20% as the upper bound for the validity of Gaussian phase approximation.

For the computation of $\frac{1}{2}\langle\Phi^2\rangle_{c,\mathrm{grad}}$ and $\frac{1}{24}\langle\Phi^4\rangle_{c,\mathrm{grad}}$ due to the fixed externally applied field gradient, we have to carry out second and fourth order differentiation numerically (see detailed discussion in Ref. (*14*)). This computation becomes less and less accurate for larger sizes of unit cell, as the error of eigenvectors gets magnified drastically. The computation for $\frac{1}{2}\langle\Phi^2\rangle_{c,\mathrm{susc}}$ and $\frac{1}{24}\langle\Phi^4\rangle_{c,\mathrm{susc}}$ due to magnetic susceptibility contrast induced field inhomogeneity is much more accurate because there is no differentiation involved. Thus, we shall focus our discussion only on the effect of the magnetic susceptibility contrast induced field inhomogeneity and its subsequent influences on the Gaussian phase approximation as well as the various approximations for the associated magnetization decay.

Figure 3 shows the second and fourth order cumulant averages as a function of $\tau$ for simple cubic arrays of touching spheres with a unit cell of length $a = 10$ $\mu$m in an externally applied field of $H_0 = 234.9$ G along the $z$ direction, where the magnetic susceptibility for the pore fluid (water) is $\chi_p = -0.7\times10^{-6}$ emu/cm$^3$ and that for the solid matrix is $\chi_m = 50\times10^{-6}$ emu/cm$^3$. We use a self diffusion coefficient for water $D = 2.5\times10^{-5}$ cm$^2$/s. The results for $\frac{1}{2}\langle\Phi^2\rangle_{c,\mathrm{susc}}$ and $-\frac{1}{24}\langle\Phi^4\rangle_{c,\mathrm{susc}}$ are shown as open circles and squares, respectively. Here the value of $\frac{1}{24}\langle\Phi^4\rangle_{c,\mathrm{susc}}$ is negative. Thus,

$$\langle\Phi^4\rangle < 3\langle\Phi^2\rangle^2, \quad [19]$$

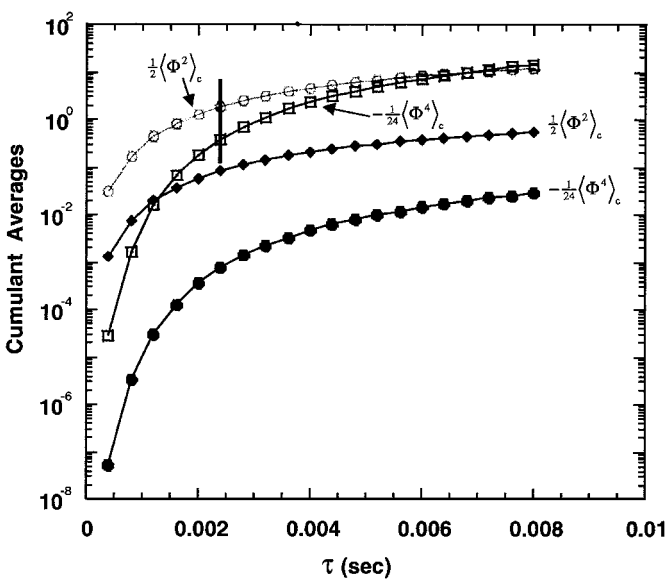


**FIG. 3.** The cumulant averages of phase of diffusing spins in a periodic porous medium of simple cubic arrays of touching spheres, as for Fig. 1.

and the large $\phi$ values are less probable than for the Gaussian phase distribution, which would have made both sides of Eq. [19] equal. Hence, the phase distribution is narrower than that of the normal Gaussian distribution. According to our definition of a threshold of 20% for the ratio, the Gaussian phase approximation is valid up to a $\tau$ of 2.4 ms. Note that the $\tau$ shown in the figure is the $\tau$ in a Hahn's spin echo experiment, not the time in a CPMG spin echo train. The results of a similar calculation using $\chi_m = 10 \times 10^{-6}$ emu/cm$^3$ and the same $\chi_p$ value as that used previously are shown as solid diamonds and circles, where the absolute value of the ratio of $\frac{1}{24}\langle\Phi^4\rangle_c/\frac{1}{2}\langle\Phi^2\rangle_c$ reaches only 5% for a $\tau$ of 8 ms.

Following such a definition of a threshold of 20% for the ratio, we have mapped out a region for the validity of Gaussian phase approximation as a function of $4\pi|\Delta\chi|\gamma H$ at various unit cell sizes for a simple cubic array of touching spheres. Results of the computation are shown in Fig. 4a. Note that from Eqs. [10] and [15], $\frac{1}{2}\langle\Phi^2\rangle_{c,susc}$ is proportional to $(4\pi|\Delta\chi|\gamma H)^2$, whereas $\frac{1}{24}\langle\Phi^4\rangle_{c,susc}$ is proportional to $(4\pi|\Delta\chi|\gamma H)^4$. Thus, the absolute value of the ratio of $\frac{1}{24}\langle\Phi^4\rangle_c/\frac{1}{2}\langle\Phi^2\rangle_c$ is proportional to $(4\pi|\Delta\chi|\gamma H)^2$ multiplied by a function related to the geometry of the porous system. For illustrative purposes, we place a scale for $|\Delta\chi|$ at 1-MHz proton Larmor frequency at the top. For 2 MHz, the scale would be expanded twice as large.

Note that for the unit cell of size $a = 10$ $\mu$m, $\frac{1}{24}\langle\Phi^4\rangle_{c,susc}$ becomes positive for $\tau$ above 40 ms. For this region, the data points are represented as solid rather than open circles. Even though the quantity

$$\langle\Phi^4\rangle_{c,susc} = \langle\Phi^4\rangle_{susc} - 3\langle\Phi^2\rangle^2_{susc} \qquad [20]$$

scales strictly as $(4\pi\Delta\chi\gamma H)^4$, the RHS of [20] is dependent on unit cell size and diffusion coefficient through their eigenvalues.

The fact that for unit cell sizes of 50 and 100 $\mu$m and the part of 10 $\mu$m that $\frac{1}{24}\langle\Phi^4\rangle_{c,susc}$ is negative reflects that phase distributions are narrower than the normal Gaussian form, because of the restricted geometry. As the unit cell size becomes smaller, the internal gradient becomes larger, its effect eventually becomes more dominant than the restriction of the geometry, and it leads to a phase distribution broader (i.e., longer tail) than the Gaussian form. Solid matrix forms other than spheres, such as sharp corners or thin flakes, often have very strong field gradients or even singularities near the high curvature points. This kind of pore fabric can easily generate a non-Gaussian phase distribution which is broader than the normal Gaussian form.

Figure 4b shows the results of Fig. 4a using the normalized total magnetization of the system at the diffusion time $\tau$ where the Gaussian approximation fails. We notice that there is a trough at intermediate values for $4\pi|\Delta\chi|\gamma H$. This is because the relative absolute value of $\frac{1}{24}\langle\Phi^4\rangle_c$ goes through a minimum as

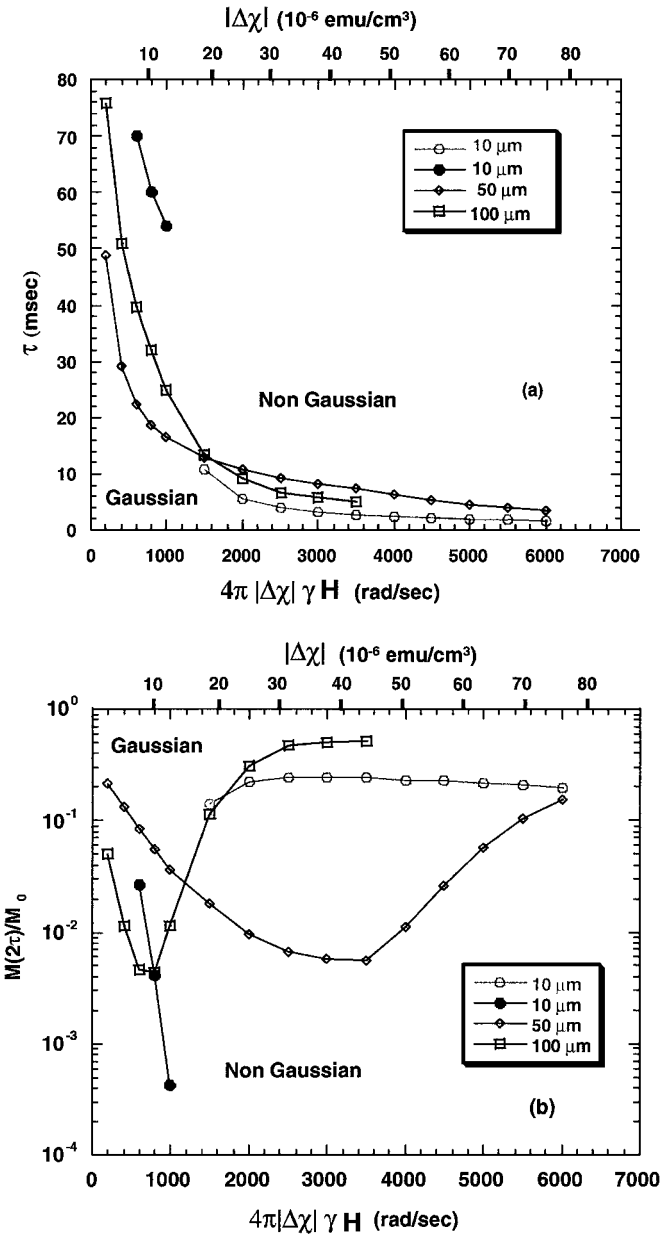


**FIG. 4.** (a) The map showing the regime where Gaussian approximation is valid for a periodic system of simple cubic arrays of touching spheres for different unit cell sizes, with an externally applied field of $H_0 = 234.9$ G (i.e., a proton Larmor frequency of 1 MHz) and a diffusion coefficient for water $D = 2.5 \times 10^{-5}$ cm$^2$/s. All data have a negative $\langle\Phi^4\rangle_{susc}$ except part of 10-$\mu$m data which have a positive $\langle\Phi^4\rangle_{susc}$ and are indicated by solid circles. (b) The same as (a) except that the $y$-axis is replaced with the total magnetization of the system at the diffusion time $\tau$ when the Gaussian approximation fails.

$4\pi|\Delta\chi|\gamma H$ goes from large values to small values. To meet the condition of the 20% threshold, the corresponding dominant term, $\frac{1}{2}\langle\Phi^2\rangle_c$, has to go to a longer diffusion time, and hence, a higher value, which leads to a lower magnetization. As $4\pi|\Delta\chi|\gamma H$ becomes even smaller, eventually both $|\frac{1}{24}\langle\Phi^4\rangle_c|$ and $\frac{1}{2}\langle\Phi^2\rangle_c$ become smaller, which leads to an increase of

magnetization at the 20% threshold at even longer diffusion time. Thus the magnetization of the system at the threshold goes through a minimum. This is true for both 50- and 100-$\mu$m cases. For the case of 10 $\mu$m, such a process actually resulted in a change of sign for $\frac{1}{24}\langle\Phi^4\rangle_c$.

## COMPARISON OF VARIOUS APPROXIMATIONS

To make a comparison between the true spin echo amplitude of the periodic porous medium computed exactly and that for various approximations, we use the same example whose field map and distributions are shown in Figs. 1 and 2; i.e., the external field is $H_0 = 234.9$ G, the unit cell has a length $a = 10\,\mu$m, $\chi_p = -0.7 \times 10^{-6}$ emu/cm$^3$ for the pore fluid, $\chi_m = 50 \times 10^{-6}$ emu/cm$^3$ for the solid matrix, and the diffusion coefficient $D = 2.5 \times 10^{-5}$ cm$^2$/s for the water. The result of such a comparison is shown in Fig. 5 where the computed spin echo amplitudes as a function of $\tau$ in a Hahn's spin echo experiment are plotted.

The true spin echo amplitude computed using the diffusion propagator is shown as solid circles along with other approximations for the magnetization. The magnetization computed using the volume averaged field gradient and the free diffusion formula, shown as open squares, gives the worst estimates, which significantly overestimate the attenuation as we expected. The magnetization obtained by integrating microdomains over the pore volume, using the averaged field gradient and the free diffusion formula for each microdomain, is shown as open diamonds. It gives good estimates at small $\tau$ initially. Then it starts to overestimate the attenuation of the magnetization until a crossover at around $\tau = 5$ ms, after which the integrated value becomes larger than the true magnetization. This type of approximation treats each volume element of integration as an isolated microdomain and neglects the field averaging effect of spin diffusion across the boundary of these microdomains. Thus, in the very beginning, when diffusion is limited, it is a good approximation. As diffusion time gets longer, it starts to overestimate the attenuation of magnetization. When the diffusion time gets even longer, the microdomains with high field gradients no longer contribute to the signal, leaving only those with low field gradients. The latter were prevented from further degradation since no spin diffusion was allowed across the boundaries between the microdomains. Thus at very long diffusion time, the integration method overestimates the magnetization.

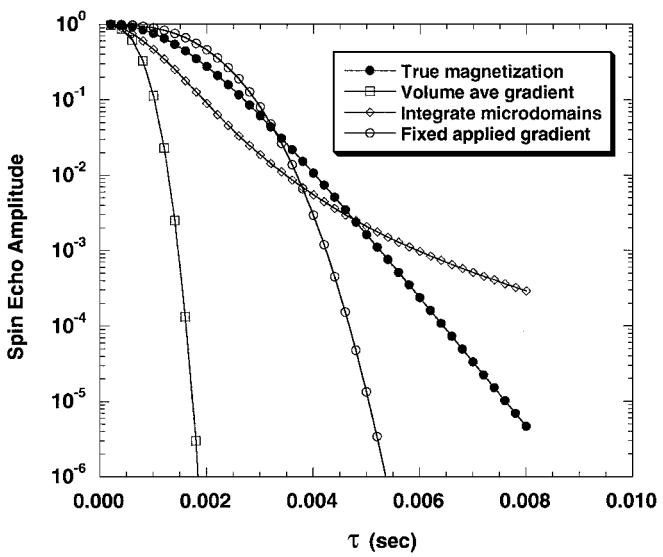


**FIG. 5.** The spin echo amplitude as a function of $\tau$ for a periodic system of simple cubic arrays of touching spheres, where the magnetic susceptibility and proton Larmor frequency values are the same as those in Fig. 1 and the bulk diffusion coefficient for water $D = 2.5 \times 10^{-5}$ cm$^2$/s. The solid circles represent the true total magnetization computed theoretically using Eq. [6]. The open squares represent the total magnetization computed using the free diffusion formula and Eq. [4], the volume averaged field gradient, as the gradient in the exponent. The open diamonds represent the total magnetization computed using the integration of microdomains, i.e., Eq. [17], where the microdomain is an element of $100 \times 100 \times 100$ mesh of a unit cell and the field gradient is the averaged field gradient of that volume element. The open circles represent the magnetization computed using the free diffusion formula with a fixed applied field gradient of 100 G/cm. The last one is plotted for comparison purposes.

The open circle in Fig. 5 is simply a magnetization using free diffusion formula with a uniform field gradient of 100 G/cm. It is plotted as a reference for discussion purposes. We note that in the beginning, the true magnetization is initially smaller than what is expected from the free diffusion in 100 G/cm. Thus it has an apparent field gradient somewhat larger than 100 G/cm. Note that the pore space has an averaged field gradient of 400 G/cm and a most probable gradient of 200 G/cm as shown in Fig. 2. The logarithm of the true magnetization displays a $\tau^3$ behavior initially. As the $\tau$ increases, the behavior becomes linear in $\tau$, as discussed by de Swiet and Sen (*3*).

If we use the free diffusion formula (Eq. [1]) as a reference, we can back calculate an effective or apparent field gradient, $g_{\text{eff}}$, from the total magnetization of the system, $M(2\tau)/M_0$, as follows,

$$\frac{M(2\tau)}{M_0} = \exp\left[-\frac{2}{3}\gamma^2 g_{\text{eff}}^2 D_p \tau^3\right], \qquad [21]$$

where the total magnetization can be either the true magnetization or the magnetization obtained from volume integration of microdomains, each domain using the free diffusion formula and the volume averaged field gradient within that microdomain. Figure 6 shows such a comparison between the back calculated apparent field gradients and the true volume average of the internal field gradients as a function of magnetic susceptibility difference $|\Delta\chi|$ at $\tau = 0.2$ ms using the same values for $\chi_p$, $D$, and $H_0$ as those used previously. Figures 7 and 8 show results of similar calculations for $\tau$ at 1 and 2 ms.

The apparent field gradient back calculated from the true magnetization is denoted by a solid circle, that from the volume integration of microdomains is denoted by a diamond, and the true volume average of the internal field gradients is denoted

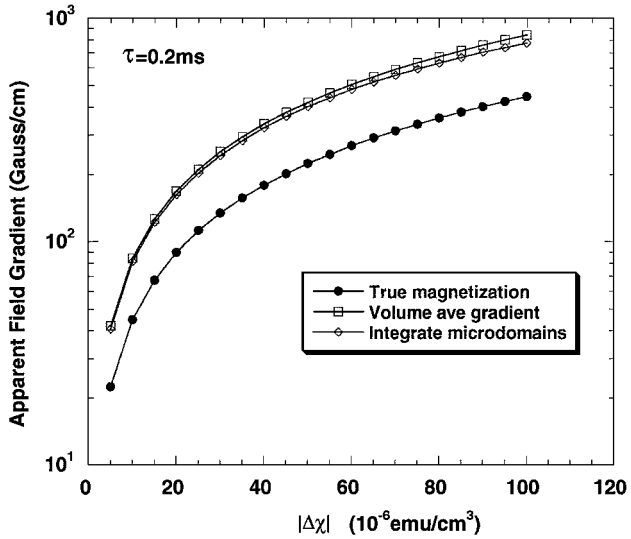


**FIG. 6.** The apparent field gradient at a proton Larmor frequency of 1 MHz as a function of magnetic susceptibility difference $|\Delta\chi|$ for a periodic system of simple cubic arrays of touching spheres (with the pores containing water with $D = 2.5 \times 10^{-5}$cm$^2$/s) for a unit cell size of 10 $\mu$m at $\tau = 0.2$ ms. The solid circles, true magnetization; open squares, volume ave gradient; and open diamonds, integrate microdomains; are the same as those defined in Fig. 5.

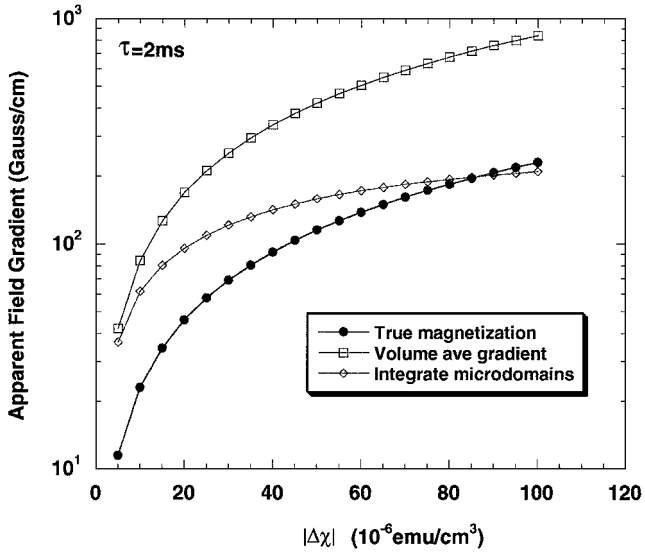


**FIG. 8.** The apparent field gradient at a proton Larmor frequency of 1 MHz as a function of magnetic susceptibility difference $|\Delta\chi|$ for a periodic system of simple cubic arrays of touching spheres (with the pores containing water with $D = 2.5 \times 10^{-5}$ cm$^2$/s) for a unit cell size of 10 $\mu$m at $\tau = 2$ ms. The solid circles, true magnetization; open squares, volume ave gradient; and open diamonds, integrate microdomains; are the same as those defined in Fig. 5.

by a square. This is just a different way of looking at the same properties which we discussed in Fig. 5, except that instead of magnetizations as functions of diffusion time $\tau$ for a fixed $|\Delta\chi|$, we are looking at apparent field gradients as functions of $|\Delta\chi|$ at a fixed $\tau$.

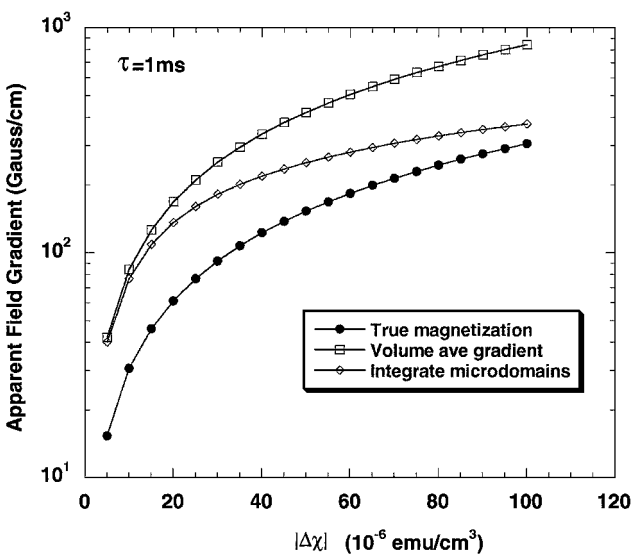


**FIG. 7.** The apparent field gradient at a proton Larmor frequency of 1 MHz as a function of magnetic susceptibility difference $|\Delta\chi|$ for a periodic system of simple cubic arrays of touching spheres (with the pores containing water with $D = 2.5 \times 10^{-5}$ cm$^2$/s) for a unit cell size of 10 $\mu$m at $\tau = 1$ ms. The solid circles, true magnetization; open squares, volume ave gradient; and open diamonds, integrate microdomains; are the same as those defined in Fig. 5.

In general, the apparent field gradient back calculated from the true magnetization is the smallest of the three, whereas the volume average of the true internal gradients should have the largest value. When the diffusion time $\tau$ is very small, such as $\tau = 0.2$ ms, the apparent field gradient calculated from the integration of magnetization over microdomains is very close to the volume average of internal gradients. The apparent field gradient of the true magnetization at $\tau = 0.2$ ms is already about a factor of three less than the other two. As the diffusion time $\tau$ increases to 1 and 2 ms, such separation becomes larger and larger.

The apparent field gradient from the integrated magnetizations over microdomains, when compared to that calculated from the true magnetization, has a crossover behavior similar to the one discussed in Fig. 5. For example, in Fig. 8 when the diffusion time $\tau = 2$ ms, the apparent field gradient calculated from integrated magnetizations over microdomains is much larger than that calculated from the true magnetization for small $|\Delta\chi|$. As $|\Delta\chi|$ increases, the internal field gradient increases. As a result, the signals from some of the microdomains diminish very quickly, resulting in a reduction of apparent field gradient. Because there is no communication between microdomains, further increase of $|\Delta\chi|$ simply leads to attenuation of signals of more microdomains, eventually resulting in an apparent field gradient smaller than that calculated from true magnetization.

Figures 9 and 10 show results of similar calculation, using the same values for $\chi_p$, $D$, and $H_0$ as those used previously, for

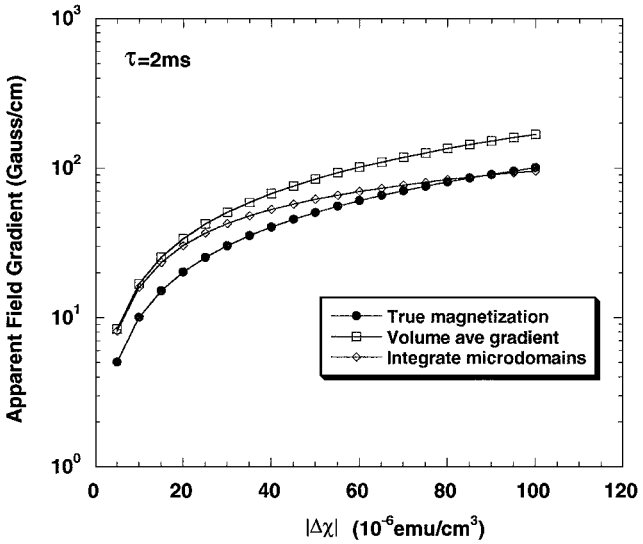


**FIG. 9.** The apparent field gradient at a proton Larmor frequency of 1 MHz as a function of magnetic susceptibility difference $|\Delta\chi|$ for a periodic system of simple cubic arrays of touching spheres (with the pores containing water with $D = 2.5 \times 10^{-5}$ cm$^2$/s) for a unit cell size of 50 $\mu$m at $\tau = 2$ ms. The solid circles, true magnetization; open squares, volume ave gradient; and open diamonds, integrate microdomains; are the same as those defined in Fig. 5.

$\tau = 2$ ms for unit cell sizes of 50 and 100 $\mu$m. Larger pore size leads to smaller internal field gradients for the same $|\Delta\chi|$. The general behavior is similar to what we have discussed previously.

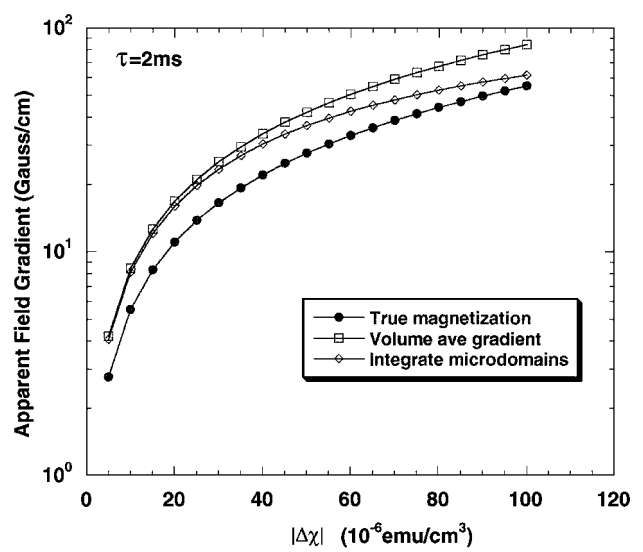


**FIG. 10.** The apparent field gradient at a proton Larmor frequency of 1 MHz as a function of magnetic susceptibility difference $|\Delta\chi|$ for a periodic system of simple cubic arrays of touching spheres (with the pores containing water with $D = 2.5 \times 10^{-5}$ cm$^2$/s) for a unit cell size of 100 $\mu$m at $\tau = 2$ ms. The solid circles, true magnetization; open squares, volume ave gradient; and open diamonds, integrate microdomains; are the same as those defined in Fig. 5.

## DISCUSSION

Experiments by Bendel (*1*) on a saturated sand–water mixture provide evidence that $\tau^3$ behavior for magnetization attenuation is not valid for large $\tau$ in restricted geometries. The magnetization shown in Fig. 4 of Bendel's paper is quite similar to the computed magnetization shown in Fig. 5 of the present work. Of course, the grain size as well as the magnetic susceptibility difference $|\Delta\chi|$ affect the $\tau$ value where the behavior departs from that for an infinite medium.

Experimental works by Brown and Fantazzini (*4*) and Borgia *et al.* (*5*) on fluid-saturated microporous porcelain samples indicate a non-Gaussian phase distribution for the spins. Their data suggest a truncated Cauchy distribution with a long tail. It is different from our geometry of touching spheres which shows a negative $\langle\Phi^4\rangle_c$, i.e., $\langle\Phi^4\rangle \leq 3\langle\Phi^2\rangle^2$, reflecting the effect of a restricted geometry. The microporous porcelain may have sharp corners which generate large local magnetic field gradient, causing a long tail in phase distribution and leading to a positive $\langle\Phi^4\rangle_c$.

The work by Hürlimann (*6, 7*) suggested a few length scales which are quite convenient for the present discussion:

1. the diffusion length, $l_D \equiv \sqrt{D_p \tau}$, where $D_p$ is the self-diffusion coefficient of the pore fluid and $\tau$ is the diffusion time,
2. the size of the pore, $l_s$, and
3. the dephasing length, $l_g \equiv (D_p/(\gamma g))^{1/3}$.

The first two length scales are commonly known. The third one, the dephasing length, can be thought of as the distance over which the spin must travel to dephase by a radian. It has the properties that it is small for large field gradient and large for small field gradient. In the process of the integration for the magnetization, however, we typically have a constant pixel size. When the pixel size is smaller than $l_g$, and at a very short diffusion time, integration of magnetization is a good approximation. However, as the diffusion time gets longer, a field averaging effect occurs on a length scale of $l_g$, whereas the pixel integration does not allow spin mixing, thus giving a higher attenuation and a higher apparent field gradient. This is illustrated in Figs. 6 through 10 for small $|\Delta\chi|$. When the pixel size is of the same order as $l_g$, then the pixel integration gives the best approximation at a diffusion time on the order of $\tau \approx l_g^2/D_p$. When the pixel size is larger than $l_g$, typically, the volume averaged field gradient is used for the pixel, thus resulting in a higher attenuation for the magnetization at short diffusion time. But as diffusion time gets longer, the isolated pixel effect will again cause overestimation of magnetization. This is illustrated in Figs. 6 through 10 in the crossover behavior of the apparent field gradient for the pixel integration compared to the true magnetization.

From the above discussion, it is apparent that one should be careful in using Eq. [1] for analyzing data obtained from a restricted geometry. There are at least three steps of consideration in analyzing the data. First of all, one should make sure that the data should be well within the regime of validity for Gaussian

approximation. Second, when the Gaussian approximation is satisfied, the effective or apparent field gradient obtained from using Eq. [1] is generally much smaller than the true volume average of the field gradients due to the field averaging effect of the spin diffusion. At this juncture, one can use a true volume averaged field gradient but a time dependent effective restricted diffusion coefficient instead of the bulk diffusion coefficient in Eq. [1] to take care of the effect. However, as diffusion time becomes longer, $\langle \Phi^4 \rangle_c$ and higher order terms become important, Gaussian approximation eventually fails, and even this modified free diffusion formula with the time dependent restricted diffusion coefficient is no longer valid.

## APPENDIX

In the following, we use Bergman's method (*18*) to compute the internal field gradients of the pore space. It is based on a Fourier-space representation of an integral equation for the static magnetic potential.

Consider a porous medium with two phases, solid matrix and pore fluid, which fills up the entire volume between two infinite parallel plates. The plates are perpendicular to the $z$-axis, and the distance between them is $L$. In magnetostatics, when the current density is zero, the governing equation reduces to the Laplace equation for a magnetic scalar potential $\varphi(\mathbf{r})$,

$$\nabla \cdot \mu(\mathbf{r}) \nabla \varphi(\mathbf{r}) = 0, \qquad [A.1]$$

where

$$\mu(\mathbf{r}) = \mu_m \theta_m(\mathbf{r}) + \mu_p \theta_p(\mathbf{r}) \qquad [A.2]$$

$$\mu(\mathbf{r}) = \mu_m \left(1 - \frac{1}{s}\,\theta_p\right), \qquad s = \frac{\mu_m}{\mu_m - \mu_p} \qquad [A.3]$$

and $\mu_m$ and $\mu_p$ are the magnetic permeability of solid matrix and pore fluid, respectively. $\theta_m$ and $\theta_p$ are the characteristic functions, having a value of either 1 or 0, which define the domain for solid matrix and pore space, respectively. The boundary conditions to be satisfied are $\varphi = 0, L$ for $z = 0, L$ on the parallel plates, respectively, and $\partial\varphi/\partial n = 0$ on the side walls.

Equation [A.1] can then be written as

$$\nabla^2 \varphi(\mathbf{r}) = \frac{1}{s} \nabla \cdot \theta_p(\mathbf{r}) \nabla \varphi(\mathbf{r}) \qquad [A.4]$$

which has a solution given by

$$\varphi(\mathbf{r}) = z - \frac{1}{s} \int dV' G(\mathbf{r}, \mathbf{r}') \nabla' \cdot \theta' \nabla' \varphi(\mathbf{r}')$$

$$= z + \frac{1}{s} \int dV' \theta_p(\mathbf{r}') \nabla' G \cdot \nabla' \varphi$$

$$\varphi = z + \frac{1}{s} \hat{\Gamma} \varphi, \qquad [A.5]$$

where

$$\hat{\Gamma} \varphi = \int dV' \theta_p(\mathbf{r}') \nabla' G(\mathbf{r}, \mathbf{r}') \cdot \nabla' \varphi(\mathbf{r}') \qquad [A.6]$$

and $G(\mathbf{r}, \mathbf{r}')$ is the Green's function which satisfies the boundary conditions and $\hat{\Gamma}$ can be shown to be a Hermitian operator defined by Eq. [A.6].

If the porous medium we consider is periodic, then the function $\psi(\mathbf{r})$, obtained by subtracting from the potential $\varphi(\mathbf{r})$ the linear function $z$

$$\psi(\mathbf{r}) \equiv \varphi - z = \frac{1}{s}(\hat{\Gamma} z + \hat{\Gamma} \psi) \qquad [A.7]$$

is also periodic. In fact, this periodic function $\psi(\mathbf{r})$ is the part of the magnetic scalar potential which gives rise to the magnetic susceptibility contrast induced field inhomogeneities. Note that the potentials we discuss here, $\psi(\mathbf{r})$ and $\varphi(\mathbf{r})$, are referring to the responses to the applied potential, $z$, which generates a unit field strength. Thus if the applied field is $H_0$ along the $z$-axis, and the local field is $H(\mathbf{r})$, then the local field deviation $\delta H_{\text{susc}}(\mathbf{r})$ due to the susceptibility contrast is given by

$$\delta H_{\text{susc}}(\mathbf{r}) \equiv H(\mathbf{r}) - H_0 = H_0 \nabla(\varphi - z) = H_0 \nabla \psi. \qquad [A.8]$$

Since $\psi(\mathbf{r})$ is periodic, we can therefore represent $\psi$ by a Fourier series

$$\psi(\mathbf{r}) = \sum_{\mathbf{g}} \psi_{\mathbf{g}} e^{i\mathbf{g}\cdot\mathbf{r}}, \qquad [A.9]$$

where the sum is over all the vectors $\mathbf{g}$ of the reciprocal lattice. The Fourier coefficients of $\psi(\mathbf{r})$ are given by

$$\psi_{\mathbf{g}} = \frac{1}{V_a} \int_{V_a} dV \psi(\mathbf{r}) e^{-i\mathbf{g}\cdot\mathbf{r}}, \qquad [A.10]$$

where $V_a$ is the volume of the unit cell of the periodic composite.

To obtain $\psi(\mathbf{r})$, we need only to compute $\psi_{\mathbf{g}}$. From Eq. [A.7], we get

$$s\psi - \hat{\Gamma} \psi = \hat{\Gamma} z. \qquad [A.11]$$

Its Fourier component can be obtained as:

$$s\psi_{\mathbf{g}} - \sum_{\mathbf{g}'} \frac{\mathbf{g} \cdot \mathbf{g}'}{|\mathbf{g}|^2}\, \theta_{\mathbf{g}-\mathbf{g}'} \psi_{\mathbf{g}'} = \frac{-i\mathbf{g} \cdot \mathbf{e}_z}{|\mathbf{g}|^2}\, \theta_{\mathbf{g}}, \qquad [A.12]$$

where $\theta_{\mathbf{g}}$ is the Fourier coefficient of $\theta_p(\mathbf{r})$ and $\mathbf{e}_z$ is the unit vector along the $z$-axis.

Let $a_{\mathbf{g}} \equiv i|\mathbf{g}|\psi_{\mathbf{g}}$ for $\mathbf{g} \neq 0$; Eq. [A.12] can be symmetrized to

$$s a_{\mathbf{g}} = \cos(\mathbf{g}, \mathbf{e_z})\theta_{\mathbf{g}} + \sum_{\mathbf{g}' \neq 0} \hat{\Gamma}_{\mathbf{g}\mathbf{g}'} a_{\mathbf{g}'}, \qquad [A.13]$$

where

$$\hat{\Gamma}_{\mathbf{g}\mathbf{g}'} \equiv \cos(\mathbf{g}, \mathbf{g}')\theta_{\mathbf{g}-\mathbf{g}'} \qquad [A.14]$$

and $(\mathbf{g}, \mathbf{e_z})$ and $(\mathbf{g}, \mathbf{g}')$ represent the angles between $\mathbf{g}$ and $\mathbf{e_z}$, and $\mathbf{g}$ and $\mathbf{g}'$, respectively.

$a_{\mathbf{g}}$ can now be solved through successive substitutions,

$$a_{\mathbf{g}} = \frac{1}{s}\cos(\mathbf{g}, \mathbf{e_z})\theta_{\mathbf{g}} + \frac{1}{s^2}\sum_{\mathbf{g}' \neq 0} \hat{\Gamma}_{\mathbf{g}\mathbf{g}'}\cos(\mathbf{g}', \mathbf{e_z}) + \frac{1}{s^3}\sum_{\mathbf{g}' \neq 0}\sum_{\mathbf{g}'' \neq 0} \hat{\Gamma}_{\mathbf{g}\mathbf{g}'}\hat{\Gamma}_{\mathbf{g}'\mathbf{g}''}\cos(\mathbf{g}'', \mathbf{e_z}) + \cdots. \qquad [A.15]$$

Since $s = (1 + 4\pi\chi_m)/4\pi(\chi_m - \chi_p)$ (where $\chi_m$ and $\chi_p$ are the magnetic susceptibility of the solid matrix and pore fluid, respectively) is typically a very large number, an excellent approximation is obtained by taking only the first term on the RHS of Eq. [A.15]

$$a_{\mathbf{g}} \equiv i|\mathbf{g}|\psi_{\mathbf{g}} \cong \frac{1}{s}\cos(\mathbf{g}, \mathbf{e_z})\theta_{\mathbf{g}}. \qquad [A.16]$$

Thus the local field deviation $\delta H_{\text{susc}}(\mathbf{r})$ due to the magnetic susceptibility contrast can be obtained as

$$\delta H_{\text{susc}}(\mathbf{r}) = H_0\frac{\partial\psi}{\partial z} \cong \frac{H_0}{s}\sum_{\mathbf{g} \neq 0}\cos^2(\mathbf{g}, \mathbf{e_z})\theta_{\mathbf{g}}e^{i\mathbf{g}\cdot\mathbf{r}}. \qquad [A.17]$$

## ACKNOWLEDGMENT

The author acknowledges Martin Hürlimann, Robert J. S. Brown, David Bergman, John Shafer, John Gardner, Gigi Zhang, Matthias Appel, and George Hirasaki for many helpful discussions and ChevronTexaco Exploration and Production Technology Co. for supporting this work.

## REFERENCES

1. P. Bendel, *J. Magn. Reson*. **86,** 509 (1990).
2. J. Zhong, R. P. Kennan, and J. C. Gore, *J. Magn. Reson.* **95,** 267 (1991).
3. T. M. de Swiet and P. N. Sen, *J. Chem. Phys.* **100,** 5597 (1994).
4. R. J. S. Brown and P. Fantazzini, *Phys. Rev. B* **47,** 14823 (1993).
5. G. C. Borgia, R. J. S. Brown, and P. Fantazzini, *Phys. Rev. E* **51,** 2104 (1995).
6. M. D. Hürlimann, K. G. Helmer, T. M. de Swiet, P. N. Sen, and C. H. Sotak, *J. Magn. Reson. A* **113,** 260 (1995).
7. M. D. Hürlimann, *J. Magn. Reson.* **131,** 232 (1998).
8. C. A. Clark, G. J. Barker, and P. S. Tofts, *J. Magn. Reson.* **141,** 522 (1999).
9. G. Q. Zhang, G. J. Hirasaki, and W. V. House, *in* "SPWLA 41st Annual Symposium," Paper AA, Dallas, TX, June 4–7 (2000).
10. K.-J. Dunn, M. Appel, J. J. Freeman, J. S. Gardner, G. J. Hirasaki, J. L. Shafer, and G. Zhang, *in* "SPWLA 42nd Annual Symposium," Houston, TX, June 17–20 (2001).
11. C. H. Neuman, *J. Chem. Phys.* **60,** 4508 (1974).
12. P. P. Mitra, P. N. Sen, L. M. Schwartz, and P. Le Doussal, *Phys. Rev. Lett.* **68,** 3555 (1992).
13. P. P. Mitra, P. N. Sen, and L. M. Schwartz, *Phys. Rev. B* **47,** 8565 (1993).
14. D. J. Bergman and K. J. Dunn, *Phys. Rev. E* **52,** 6515 (1995).
15. D. J. Bergman, *J. Phys. C* **12,** 4947 (1979).
16. D. J. Bergman, *in* "Les Méthodes de l'Homogénéisation: Théorie et. Applications en Physique" pp. 1–128, École d'Été d'Analyse Numérique, Édition Eyrolles, Paris (1985).
17. D. J. Bergman, *Ann. Phys.* **138,** 78 (1982).
18. D. J. Bergman and K. J. Dunn, *Phys. Rev. B* **45,** 13262 (1992).
19. K. J. Dunn and D. J. Bergman, *J. Chem. Phys.* **102,** 3041 (1995).